



Research paper

Comparison of tissue distribution of a PEGylated Radix Ophiopogonis polysaccharide in mice with normal and ischemic myocardium

Xiao Lin^{a,b}, Zhuo-Jun Wang^b, Shuo Wang^a, Lan Shen^b, Yi Feng^{a,*}, Ke-Feng Ruan^a, De-Sheng Xu^{c,*}^a Engineering Research Center of Modern Preparation Technology of TCM of Ministry of Education, Shanghai University of Traditional Chinese Medicine, Shanghai, PR China^b College of Chinese Materia Medica, Shanghai University of Traditional Chinese Medicine, Shanghai, PR China^c Shuguang Hospital, Shanghai University of Traditional Chinese Medicine, Shanghai, PR China

ARTICLE INFO

Article history:

Received 9 May 2011

Accepted in revised form 8 July 2011

Available online 19 July 2011

Keywords:

Radix Ophiopogonis polysaccharide

PEGylation

Tissue distribution

EPR effect

Myocardial ischemia

ABSTRACT

PEGylation was found to be a promising approach to improve the anti-myocardial ischemic activity of Radix Ophiopogonis polysaccharide (ROP) by prolonging its retention in plasma. To fully evaluate the effectiveness and safety of this strategy, the tissue distribution of PEGylated ROP was investigated in this study. A long-circulating and bioactive PEGylated ROP with 1.04 mol 20-kDa mPEG per mol ROP ($_{1.04}P_{20k}$ -R) was prepared by a moderate coupling reaction between the hydroxyl-activated ROP and the amino-terminated mPEG. Its tissue distribution in mice with normal and ischemic myocardium was studied and compared with ROP. The results show that the descending order of tissue distribution of $_{1.04}P_{20k}$ -R ranked by AUC was kidney, lung, heart, liver, and brain in normal mice and kidney \approx lung \approx heart, liver and brain in mice with myocardial ischemia. With the exception of the heart, myocardial ischemia did not cause obvious changes in the distribution of $_{1.04}P_{20k}$ -R in the other tissues studied. Owing to the enhanced permeability and retention effect caused by ischemia, the AUC of $_{1.04}P_{20k}$ -R in ischemic hearts was approximately 1.6-fold greater than in normal hearts. Compared with ROP in rats, the distribution tendency of $_{1.04}P_{20k}$ -R in mouse kidney, brain, and lung was reduced by approximately 42, 1.6, and 1.3 times, respectively, whereas it was increased by approximately 1.3-fold in the liver. The results of this study are highly instructive for the further pharmaceutical development of PEGylated ROP.

© 2011 Elsevier B.V. All rights reserved.

1. Introduction

Covalent attachment of polyethylene glycol (PEG) polymer chain(s) to a medicinal agent (a process known as 'PEGylation') represents a promising approach that may significantly improve drug pharmacokinetics and, in turn, pharmacodynamics [1,2]. After PEGylation, the drug may achieve a prolonged body residence, optimized tissue distribution, decreased adverse effects, and an increased resistance to degradation [3,4]. These advantages generally improve patient compliance. Compared with PEGylation of peptides and proteins, which has already led to approximately ten marketed products [5], PEGylation of carbohydrate-based drugs is relatively new and rarely reported, although there are some reports regarding the application of PEGylated polysaccharides as drug carrier [6–8] or surfactant [9].

Radix Ophiopogonis polysaccharide (ROP), a natural graminan-type fructan with a molecular weight of approximately 5 kDa, had

been found to have an anti-myocardial ischemic activity [10,11]. However, its rapid renal excretion following intravenous administration significantly limits its efficacy and clinical application [12]. In a previous study [13], it was found that with proper design, PEGylated ROP that is both bioactive and long circulating in the blood could be obtained. For example, the one with a PEG (20 kDa) grafting degree of approximately 1 was found to have a 47-fold increase in elimination half-life while preserving approximately 74% of ROP bioactivity. In another study, it was found that the accumulation of ROP (~ 2 nm) in the hearts of rats with experimental myocardial ischemia was approximately 2.2-fold higher than that in normal rat hearts [14], suggesting that the enhanced permeability and retention (EPR) effect caused by ischemia [15,16] can surpass the negative effect of the decreased blood flow on drug distribution during ischemia. However, the use of the EPR effect is, to a large extent, limited by the rapid renal excretion of ROP, making the increase far from ideal. Could PEGylated ROP that is long circulating in the blood, has well-preserved bioactivity and is much smaller (~ 10 nm) than colloidal drug delivery systems, such as the one mentioned above, still effectively use the EPR effect to passively target ischemic myocardia? Will PEGylation and myocardial ischemia lead to changes in drug distribution in important non-targeting tissues? This study was carried out to answer these questions, with the aim of providing useful information for the

* Corresponding authors. Engineering Research Center of Modern Preparation Technology of TCM of Ministry of Education, Shanghai University of Traditional Chinese Medicine, Shanghai 201203, PR China. Tel./fax: +86 21 50796201 (Y. Feng), Shuguang Hospital, 185 Pu An Road, Shanghai 200021, PR China. Tel./fax: +86 21 53825761 (D.-S. Xu).

E-mail addresses: yy090503@163.com (Y. Feng), shutcmxds@163.com (D.-S. Xu).

comprehensive evaluation of the effectiveness and safety of PEGylating ROP in this manner.

2. Materials and methods

2.1. Materials and animals

ROP was prepared according to the method used in a previous report [17]. Linear amino-terminated polyethylene glycol methyl ether (mPEG-NH₂), which has a molecular weight of 20 kDa, was purchased from Jenkem Technology Co., Ltd. (Beijing, China). *p*-Nitrophenyl chloroformate and 4-*N,N*-(dimethylamino) pyridine (DMAP) were purchased from Fluka (Buchs, Germany). Fluorescein isothiocyanate (FITC) was purchased from Sigma (St. Louis, MO, USA). Extra dry dimethyl sulfoxide (DMSO) was purchased from Acros Organics (Geel, Belgium). Dichloromethane (CH₂Cl₂) and pyridine from Sinopharm Chemical Reagent Co., Ltd. (Shanghai, China) were dried over CaH₂ and KOH, respectively, and distilled before use. All other chemicals were of reagent grade and purchased from commercial sources.

KM mice (approximately 4–5 weeks old) were supplied by the Lab Animal Center of Shanghai University of TCM. They were kept in an environmentally controlled breeding room for 4 days before starting the experiments and fed with standard laboratory food and given water *ad libitum*. The Animal Ethical Experimentation Committee of Shanghai University of TCM, according to the requirements of the National Act on the Use of Experimental Animals (PR China), approved all procedures of the animal experiments.

2.2. Preparation of FITC-labeled PEGylated ROP

A PEGylated ROP was synthesized through a coupling reaction between hydroxyl-activated ROP and amino-terminated mPEG [13]. The reaction's molar ratio of hydroxyl-activated ROP (degree of activation: 13%) to 20-kDa mPEG-NH₂ was set at 5:1 in this study, so that a conjugate with a PEG grafting number approaching 1.0 was prepared. Characterization of the conjugate was carried out by high-performance gel permeation chromatography (HPGPC) in conjunction with anthrone-sulfuric acid colorimetry [13]. The HPLC system consisted of a Waters liquid chromatograph and a Waters 2414 refractive index detector (Milford, USA). After characterization, the conjugate was labeled with FITC according to a method previously used [13].

2.3. Analytical conditions and sample pretreatment procedure

The assay system consisted of an Agilent 1200 series HPLC with a fluorescence detector set at λ_{ex} 495 nm and λ_{em} 515 nm. Samples were separated by HPGPC using an 8.0 × 300-mm Shodex OHpak SB-803 HQ column. The eluent was 0.1 M phosphate buffer (pH 7.4), delivered at a flow rate of 0.5 ml/min. The chromatographic procedures were performed at 30 °C.

To a 100- μ l portion of each tissue homogenate, 40 μ l of 1 M perchloric acid was added. The mixture was vortexed and then centrifuged at 10,000 rpm for 1 min to precipitate denatured proteins. The heart samples were left to stand for 2 h before centrifugation. The supernatant was neutralized by the addition of 30 μ l of 1 M NaOH. After centrifugation at 10,000 rpm for 1 min again, the supernatant was assayed by the method described above.

2.4. Preparation of standard and quality control samples

Stock solution of the FITC-labeled conjugate in phosphate buffer (pH 7.4) at a concentration of 10 mg/ml was prepared. A series of

standard solutions with a concentration range of 10–1000 μ g/ml were then obtained by further dilution of stock solution with phosphate buffer (pH 7.4).

To prepare the standard calibration samples, an aliquot of each standard solution placed in a 1.5-ml centrifuge tube was blown dry with nitrogen gas followed by the addition of 100 μ l blank tissue homogenates. After being thoroughly homogenized by vortexing, the mixture was then treated according to the sample pretreatment procedure described above. The final standard tissue concentrations were 2–486 μ g/ml for the conjugate. The quality control (QC) samples, which were used in method validation, were prepared in the same way as the standard calibration samples.

2.5. Tissue distribution study

Mice with acute myocardial ischemia induced by isoprenaline (20 mg/kg daily by intraperitoneal injection for three consecutive days), and normal mice, were given a single intravenous dose (170 mg/kg) of the FITC-labeled conjugate via the tail vein and killed at predefined times (0.5, 1, 4, 12, and 24 h postdose). Various tissues (heart, kidney, liver, brain, and lung) were immediately harvested, kept in saline solution to remove the blood and contents, blotted on filter paper, and then weighed for wet weight. After homogenization using a 3-fold volume of 0.1 M phosphate buffer (pH 7.4), tissue samples were stored at –20 °C until assay.

2.6. Data analysis

Data were expressed as means \pm SD. Statistical analyses were assessed using Student's *t*-test. Statistically significant differences were indicated by *p* values of <0.05.

3. Results and discussion

3.1. Characterization of PEGylated ROP and FITC-labeled PEGylated ROP

Since the ¹H NMR or FTIR method was inapplicable for the characterization of the conjugate prepared in this study due to the lack of anomeric protons and carbamate bonds in its structure, it was characterized by HPGPC coupled with the carbohydrate-specific anthrone-sulfuric acid colorimetry. PEGylation was confirmed mainly by (i) the left-shifted HPGPC peak and increased polydispersity index of the conjugate when compared with the mPEG agent used and, more importantly, (ii) the positive chromogenic reaction between the anthrone-sulfuric acid reagent and the eluate corresponding to the HPGPC peak for the conjugate. The calculated apparent weight-average molecular mass for the conjugate was 23.8 kDa. As the calibrated apparent weight-average molecular masses for ROP and 20-kDa mPEG were 2.06 and 21.0 kDa, respectively, the grafting number for the conjugate was 1.04 mol 20-kDa mPEG per mol ROP. For convenience, the conjugate is therefore denoted as _{1.04}P_{20k}-R in the following description. Owing to the lack of direct and specific microassay methods for both ROP and PEG, _{1.04}P_{20k}-R was prelabeled with FITC to study its tissue distribution in mice. After FITC labeling, no remarkable differences in the elution position and the peak shape of the conjugate were observed, indicating that its chain was stable during reaction. Although the FITC label assumes a negative charge at physiological pH, the pharmacokinetics and tissue distribution of FITC-labeled _{1.04}P_{20k}-R were believed to be similar to those of unlabeled _{1.04}P_{20k}-R in terms of both the less than 0.3% volume of FITC in the conjugate (approximately 0.17 mol FITC per mol _{1.04}P_{20k}-R) and the strong hydrophilic shielding effect of the PEG moiety. Actually, it had been found in previous studies that the

pharmacokinetics of FITC-labeled ROP following intravenous administration was similar to that of ROP [12,14].

3.2. Method validation

HPGPC coupled with FITC prelabeling was used in this study to determine $^{1,04}\text{P}_{20\text{k}}\text{-R}$ in various mouse tissues. The method was validated for specificity, linearity, precision, accuracy, sensitivity, recovery, and stability. The results obtained (see below) demonstrated that the method was accurate, specific, and stable.

The specificity of the method was assessed by comparing chromatograms of blank biosamples from different mice with those of blank biosamples spiked with standard solutions and the biosamples collected after intravenous administration of FITC-labeled $^{1,04}\text{P}_{20\text{k}}\text{-R}$. The results show that the determination was specific for $^{1,04}\text{P}_{20\text{k}}\text{-R}$ (Fig. 1). The typical retention times for FITC-labeled $^{1,04}\text{P}_{20\text{k}}\text{-R}$ and ROP were approximately 15.1 and 19.4 min, respectively. HPGPC separates analytes according to their hydrodynamic volumes, and thus, a change in the molecular weight of analytes will lead to a change in their HPGPC peak shape and location. This makes HPGPC a suitable technique for monitoring possible

Table 1

Linearity and sensitivity of detection for FITC-labeled $^{1,04}\text{P}_{20\text{k}}\text{-R}$ in mouse tissues by HPGPC ($n = 6$).

Tissues	Standard curves	Correlation coefficients	Linear ranges ($\mu\text{g/ml}$)	DL ($\mu\text{g/ml}$)	QL ($\mu\text{g/ml}$)
Kidney	$Y = 0.024C - 0.019$	0.9995	2.0–162.0	1.16	3.87
Lung	$Y = 0.021C + 0.001$	0.9990	6.0–486.0	2.07	7.14
Heart	$Y = 0.029C - 0.021$	0.9995	3.0–243.0	1.06	3.53
Liver	$Y = 0.016C - 0.027$	0.9996	5.0–405.0	1.92	6.40
Brain	$Y = 0.024C + 0.010$	0.9989	2.0–162.0	1.30	4.44

degradation of macromolecular analytes after dosing. In this study, no obvious breakage of $^{1,04}\text{P}_{20\text{k}}\text{-R}$ was observed postdose.

Standard curves of the peak height (Y) to the concentration (C) were constructed using the $1/C$ or $1/CC$ weighted linear least squares regression model. Linearity was evident over the concentration range studied in various tissues, with correlation coefficients larger than 0.998 (Table 1). The detection limit (DL) and quantification limit (QL) of the method calculated from the signal-to-noise ratio (DL and QL correspond to the 3- and 10-fold of the noise level, respectively) were approximately 1–2 $\mu\text{g/ml}$ and 3–7 $\mu\text{g/ml}$, respectively (Table 1).

The precision and accuracy of the method were examined by adding known amounts of FITC-labeled $^{1,04}\text{P}_{20\text{k}}\text{-R}$ to blank mouse tissues. The results show that the interday and intraday precisions of analysis were not more than 11.1%, and assay accuracy ranged from 93.3% to 114.3% (Table 2). The absolute recoveries of FITC-labeled $^{1,04}\text{P}_{20\text{k}}\text{-R}$ were tested at three QC levels by comparing the calculated concentrations from pretreated tissue samples with those found by direct injection of standard solutions at the same concentration, which were found to be between 57.9% and 78.1% (Table 2). Analysis of biosamples tested for storage and freeze/thaw stability consistently produced results that were nearly identical to those of freshly prepared biosamples (the relative error was within $\pm 15\%$).

A notable phenomenon was observed when the pretreatment procedure was established for heart tissues. FITC-labeled $^{1,04}\text{P}_{20\text{k}}\text{-R}$ was undetectable by this method if heart homogenates were centrifuged immediately after the addition of perchloric acid. This was believed to be attributable to specific endogenous macromolecule(s) in heart tissues. Further study revealed that a satisfactory solution to this problem was to leave the samples to stand for a

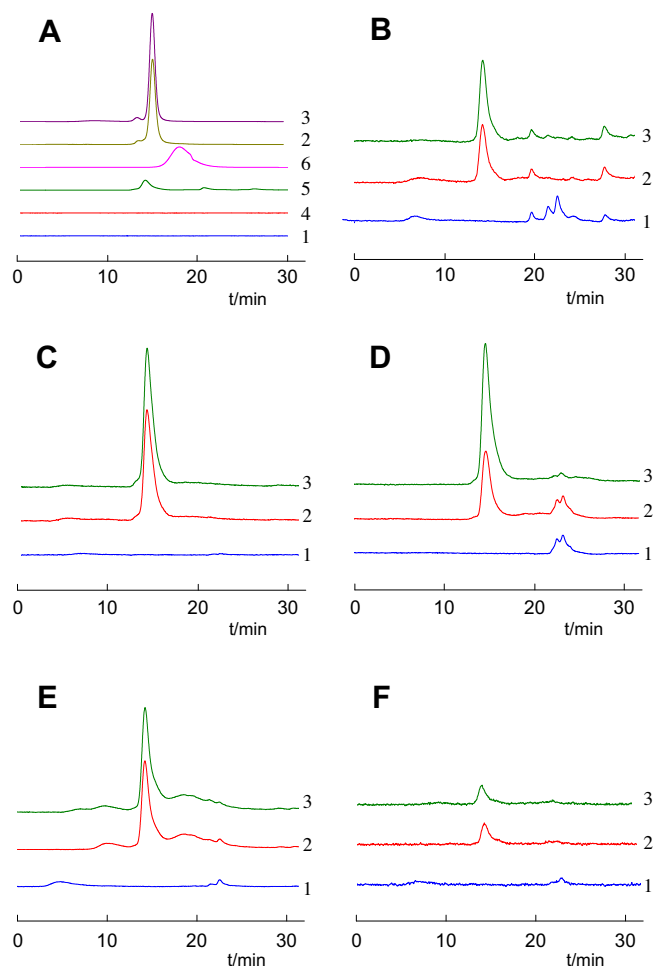


Fig. 1. Representative chromatograms for the determination of FITC-labeled $^{1,04}\text{P}_{20\text{k}}\text{-R}$ in plasma (A) and various tissues (B: kidney; C: lung; D: heart; E: liver; F: brain) by HPGPC. 1: Blank plasma or tissue; 2: Blank plasma or tissue spiked with standard FITC-labeled $^{1,04}\text{P}_{20\text{k}}\text{-R}$ solution; 3: Plasma or tissue sample collected after intravenous administration of FITC-labeled $^{1,04}\text{P}_{20\text{k}}\text{-R}$; 4: Blank urine; 5: Urine sample collected at 12 h after intravenous administration of FITC-labeled $^{1,04}\text{P}_{20\text{k}}\text{-R}$; and 6: Blank plasma spiked with FITC-labeled ROP. (For interpretation of the references to colour in this figure legend, the reader is referred to the web version of this article.)

Table 2

Recovery, precision, and accuracy for the assay of FITC-labeled $^{1,04}\text{P}_{20\text{k}}\text{-R}$ in mouse tissues by HPGPC ($n = 5$).

Tissues	Added concentration ($\mu\text{g/ml}$)	Recovery (%)	Accuracy (%)	Precision R.S.D. (%)	
				Intraday	Interday
Kidney	5	73.7 ± 4.0	107.5 ± 5.9	5.39	7.36
	50	67.0 ± 2.6	94.9 ± 3.7	3.92	4.69
	100	62.5 ± 3.0	95.8 ± 4.6	4.76	4.87
Lung	10	68.7 ± 3.3	104.2 ± 3.6	3.46	6.52
	50	66.3 ± 4.4	99.5 ± 2.8	2.85	5.72
	100	69.4 ± 5.4	101.2 ± 1.6	1.58	6.91
Heart	3	57.9 ± 6.3	114.3 ± 6.4	5.75	8.06
	10	64.8 ± 3.7	107.5 ± 11.9	11.1	10.1
	20	58.4 ± 2.7	98.2 ± 9.2	9.39	7.55
Liver	10	77.9 ± 5.2	98.0 ± 3.0	6.65	7.91
	20	78.1 ± 1.5	112.0 ± 2.1	1.88	1.97
	50	78.0 ± 1.9	102.0 ± 2.5	2.46	3.61
Brain	5	67.2 ± 5.6	100.0 ± 5.9	6.00	7.71
	10	62.1 ± 4.1	93.3 ± 4.8	5.14	4.97
	50	65.6 ± 1.4	105.8 ± 6.7	6.29	6.09

certain period of time after the addition of perchloric acid and before centrifugation. Standing for 0.5 h and 2 h improved the recovery to 50% and 60%, respectively, but no further improvement was observed with increasing standing time from 2 h up to 48 h. Therefore, at least 2 h standing after the addition of perchloric acid was necessary for heart samples. For other tissues studied, no meaningful differences in recovery were observed between samples left to stand and those centrifuged immediately; thus, standing before centrifugation was unnecessary for those tissues. FITC-labeled $_{1.04}P_{20k}$ -R was shown to be stable under the ultimately established pretreatment conditions.

3.3. Comparison of tissue distribution

The levels of $_{1.04}P_{20k}$ -R in several important tissues from normal mice and mice with myocardial ischemia at 0.5, 1, 4, 12, and 24 h after intravenous dosing were determined and listed in Table 3. The results show that (i) the highest level of $_{1.04}P_{20k}$ -R was observed in all of the tissues studied at 0.5 h postdose (Fig. 2), (ii) $_{1.04}P_{20k}$ -R was undetectable in the brain at and beyond 4 h, and, most particularly, (iii) with the exception of the heart, myocardial ischemia did not cause obvious changes in the distribution of $_{1.04}P_{20k}$ -R in the other tissues studied (Figs. 2 and 3). The descending order of tissue distribution of $_{1.04}P_{20k}$ -R ranked by AUC was kidney, lung, heart, liver, and brain in normal mice and kidney \approx lung \approx heart, liver, and brain in mice with myocardial ischemia. On the basis of AUC, the distribution of $_{1.04}P_{20k}$ -R in ischemic hearts was approximately 1.6-fold higher than in normal hearts, indicating that its hydrodynamic volume was still small enough to ensure that the EPR effect caused by ischemia [15,16] can surpass the negative effect of the decreased blood flow on drug distribution during ischemia. The difference may be underestimated because there may be more residual blood in normal myocardium than in ischemic myocardium. This might result in a severe overestimation of $_{1.04}P_{20k}$ -R levels in normal myocardium. The mechanism of the EPR effect in ischemic regions may involve [15,16,18] (i) increased capillary permeability by the active production of vascular permeability factors; (ii) the opening of additional collaterals of myocardial vasculature; (iii) membrane phospholipid degradation and resultant membrane dysfunction by cytosolic and mitochondrial Ca^{2+} accumulation and (iv) prolongation of retention time by a decrease in blood flow (the ratio for blood flow in the normal to ischemic region was approximately 10:1). Compared with ROP, the levels of $_{1.04}P_{20k}$ -R in normal and ischemic mouse myocardium were increased by approximately 22.2- and 20.5-fold at 1 h after intravenous dosing, respectively (Table 3).

Tissue distribution tendency of ROP in rats [14], calculated as the ratio of tissue AUC_{0-t} to plasma AUC_{0-t} , was compared with that of $_{1.04}P_{20k}$ -R in normal mice and mice with myocardial ischemia (Fig. 3). The significantly higher accumulation of ROP in kidney than in the other tissues is consistent with its rapid renal excretion, which reduces its efficacy and duration of activity. Compared with ROP in rats, the distribution tendency of $_{1.04}P_{20k}$ -R in mouse kidney, brain, and lung was reduced by approximately 42, 1.6, and 1.3 times, respectively, whereas it was increased by approximately 1.3-fold in the liver. Significantly decreased distribution tendency in the kidney, together with slightly changed distribution tendency in other tissues, increased the mean retention time of $_{1.04}P_{20k}$ -R in plasma by approximately 34-fold. As a modifying polymer, PEG has unique advantages, which are as follows: (i) the lack of immunogenicity, antigenicity, and toxicity; (ii) its high solubility in water and in many organic solvents; (iii) the high hydration and flexibility of the chain; and (iv) its approval by the FDA for human use in injectable formulations [1,2]. However, it is also important to recognize that PEG itself may possess antigenic and immunogenic properties. This has led to decreased effectiveness of treatment with some PEGylated therapeutics [19] and might be the reason for the slightly increased distribution tendency of $_{1.04}P_{20k}$ -R in mouse liver when compared with that of ROP in rat liver. In contrast, the decreased vascular permeability of $_{1.04}P_{20k}$ -R caused by its increased hydrodynamic volume in blood might be the reason for its slightly decreased distribution tendency in mouse brain and lung. However, since the distribution results for ROP and $_{1.04}P_{20k}$ -R were obtained in rats and mice, respectively, it is also possible that the above-mentioned slight differences in distribution were simply caused by species differences.

Regardless of molecular weights, PEGs are excreted predominantly unchanged by the kidneys [20], which means that this organ is likely to be exposed to the highest burden of PEG. Generally, there is little or no toxicity associated with PEG; however, when toxicity is observed, it is most frequently associated with the kidneys and, more particularly, associated with ultrastructural vacuolation of the proximal renal tubules [21]. Metabolism of the hydroxyl group on PEG to the corresponding acid or diacid metabolite does occur; however, this is rapidly reduced as the molecular weight increases, such that at molecular weights of 6 kDa, less than 4% of the dose was potentially metabolized [20]. Moreover, the use of PEG methyl ethers (mPEGs) in PEGylation is likely to further lower metabolism and thus toxicity because of the lack of hydroxyl groups required to initiate this metabolism. Generally, it is believed that the mechanism by which PEG is

Table 3
Distribution of FITC-labeled $_{1.04}P_{20k}$ -R in tissues after a single intravenous dose (170 mg/kg) in mice ($n = 4-5$).

Tissue	Group	Concentration ($\mu\text{g/ml}$)					AUC (mg h/l)
		0.5 h	1 h ^a	4 h	12 h	24 h	
Kidney	Normal	89.5 \pm 19.7	27.7 \pm 5.90	18.7 \pm 5.42	10.7 \pm 2.60	5.35 \pm 0.75	351
	Ischemic	96.0 \pm 15.7	26.4 \pm 1.78	17.1 \pm 0.74	10.3 \pm 3.61	3.80 \pm 1.53	332
Lung	Normal	92.9 \pm 11.6	26.5 \pm 8.87	13.3 \pm 3.69	10.4 \pm 1.19	5.82 \pm 1.40	323
	Ischemic	86.1 \pm 23.6	25.1 \pm 7.16	15.5 \pm 6.16	12.0 \pm 1.99	5.28 \pm 1.46	339
Heart	Normal	36.5 \pm 6.76	24.0 \pm 2.16	13.2 \pm 2.23	6.08 \pm 1.26	2.78 \pm 0.58	210
	Ischemic	65.7 \pm 9.59**	35.9 \pm 0.83**	20.9 \pm 2.48**	10.2 \pm 2.11**	3.98 \pm 0.59*	337
Liver	Normal	24.5 \pm 4.64	5.46 \pm 0.85	3.72 \pm 0.40	9.10 \pm 1.59	6.29 \pm 1.44	175
	Ischemic	26.0 \pm 4.67	4.93 \pm 0.20	3.16 \pm 0.41	9.70 \pm 2.08	5.62 \pm 0.44	174
Brain	Normal	4.59 \pm 0.80	1.16 \pm 0.09	ND	ND	ND	7.36
	Ischemic	4.00 \pm 0.37	1.00 \pm 0.14	ND	ND	ND	6.96
Plasma	Normal	1872 \pm 19.7	780 \pm 146	330 \pm 83.6	162 \pm 14.3	42.9 \pm 15.9	6417
	Ischemic	1827 \pm 55.7	812 \pm 121	350 \pm 50.1	180 \pm 38.0	42.3 \pm 16.7	6730

ND, undetectable; AUC, area under the curve; * $P < 0.05$, ** $P < 0.01$, compared with hearts taken from normal mice.

^a The levels of ROP in normal and ischemic mouse hearts at 1 h after intravenous dosing of 170 mg/kg of FITC-labeled ROP were $1.08 \pm 0.15 \mu\text{g/ml}$ and $1.75 \pm 0.51 \mu\text{g/ml}$, respectively.

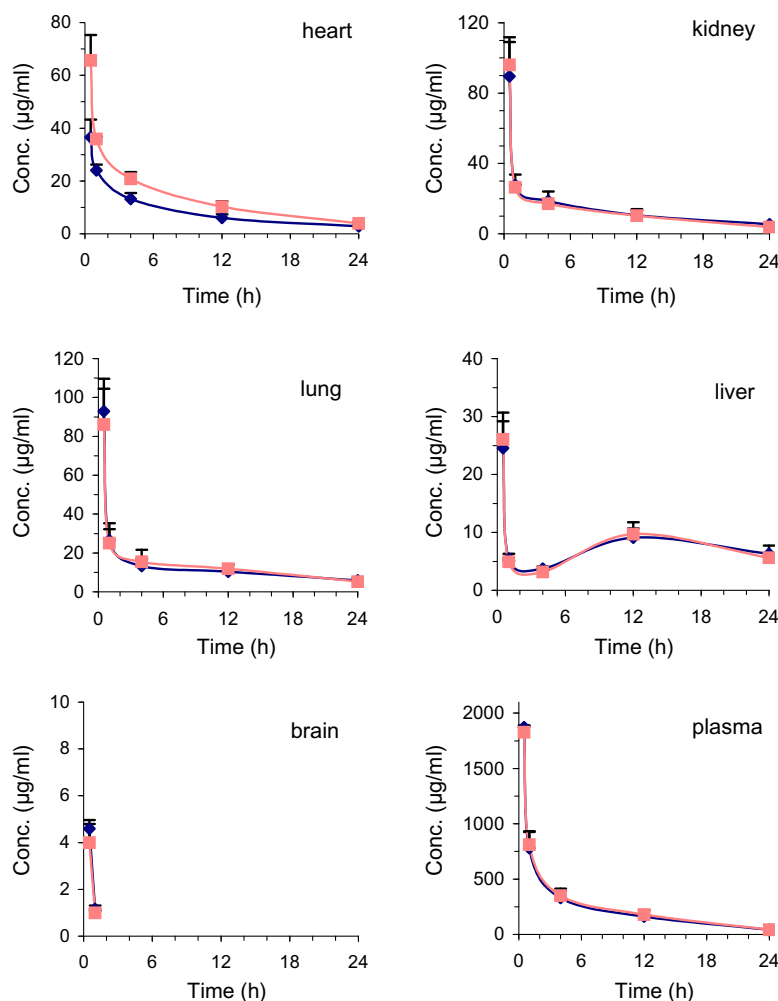


Fig. 2. Tissue and plasma FITC-labeled $1,04P_{20k}\text{-R}$ level versus time profiles following intravenous administration at 170 mg/kg to normal mice (diamonds) and mice with myocardial ischemia (squares). Each data point represents the mean \pm SD. (For interpretation of the references to colour in this figure legend, the reader is referred to the web version of this article.)

released from PEGylated proteins is probably by the degradation of the protein portion of the conjugates by proteases and similar enzymes, which was primarily occurred in the liver as well as in the kidney following the reabsorption of conjugates in the kidney tubules [22,23]. In this study, no obvious breakage of $1,04P_{20k}\text{-R}$ was observed in plasma and in the tissues studied. The sparse distribution of $1,04P_{20k}\text{-R}$ in the liver and kidney also suggests little, if any, toxicity.

Ischemic heart disease is a serious health issue. Although there are many kinds of anti-ischemic drugs, most of them lack in tissue specificity, which, together with a markedly reduced blood circulation in ischemic regions, often leads to quite low drug distribution in the targets. Myocardial ischemia can cause many pathophysiological changes, including the enhanced permeability of endothelial cell membranes, upregulation of various cell adhesion molecules on the endothelium, exposure of intracellular antigenic components, and decreased pH in ischemic areas [24–26]. To date, some of these changes have been exploited, with limited success, to allow the passive, active, and physicochemical targeting of diagnostic or therapeutic drugs to myocardial ischemic areas [24–26]. However, more effective delivery strategies are still eagerly needed. In this study, a strategy based on PEGylation and the EPR effect was confirmed to be effective in increasing the distribution of ROP in ischemic hearts by approximately 30-fold. Further improvement could be achieved if this strategy is combined with active targeting. In addition, it was found that after being adminis-

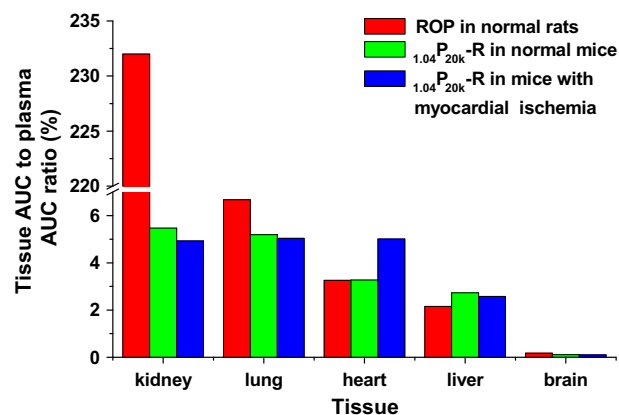


Fig. 3. Tissue distribution tendency of ROP and $1,04P_{20k}\text{-R}$ after intravenous administration. (For interpretation of the references to colour in this figure legend, the reader is referred to the web version of this article.)

tered intravenously at a dose of 80 mg/kg to rats with acute myocardial ischemia caused by coronary artery ligation, $1,04P_{20k}\text{-R}$ could effectively reduce the serum level of lactate dehydrogenase in group with the acute myocardial ischemia from $11,324 \pm 1432$ U/L to 5612 ± 1069 U/L ($n = 5$, $P < 0.01$), which approaches the

normal levels of 4905 ± 1135 U/L for the sham group ($n = 6$, $P > 0.05$). These results, together with those obtained in a previous study [13], indicate that PEGylation is a promising approach for improving the clinical efficacy of ROP and patient compliance by prolonging its retention in plasma and increasing its distribution in targets.

4. Conclusion

The descending order of tissue distribution of $_{1.04}P_{20k}$ -R ranked by AUC was kidney, lung, heart, liver and brain in normal mice and kidney \approx lung \approx heart, liver, and brain in mice with myocardial ischemia. With the exception of heart, myocardial ischemia did not cause obvious changes in the distribution of $_{1.04}P_{20k}$ -R in the other tissues studied. The AUC of $_{1.04}P_{20k}$ -R in ischemic hearts was approximately 1.6-fold larger than that in normal hearts. The results of this study provide useful information for the comprehensive evaluation of the effectiveness and safety of PEGylated ROP.

Acknowledgements

This work was supported by the National Natural Science Foundation of China (81073065), the Shanghai Rising-Star Program (07QA14050), the Shanghai Science and Technology Committee Item (09DZ1973000), the Key Discipline Project of Shanghai Education Committee (J50302), and the Xinglin Scholar Program of Shanghai University of TCM.

References

- [1] J.S. Kang, P.P. DeLuca, K.C. Lee, Emerging PEGylated drugs, *Expert Opin. Emerg. Drugs* 14 (2009) 363–380.
- [2] J.M. Harris, R.B. Chess, Effect of PEGylation on pharmaceuticals, *Nat. Rev. Drug Discov.* 2 (2003) 214–221.
- [3] Y. Nojima, Y. Suzuki, K. Yoshida, F. Abe, T. Shiga, T. Takeuchi, A. Sugiyama, H. Shimizu, A. Sato, Lactoferrin conjugated with 40-kDa branched poly(ethylene glycol) has an improved circulating half-life, *Pharm. Res.* 26 (2009) 2125–2132.
- [4] R.B. Pepinsky, D.J. LePage, A. Gill, A. Chakraborty, S. Vaidyanathan, M. Green, D.P. Baker, E. Whalley, P.S. Hochman, P. Martin, Improved pharmacokinetic properties of a polyethylene glycol-modified form of interferon-beta-1a with preserved in vitro bioactivity, *J. Pharmacol. Exp. Ther.* 297 (2001) 1059–1066.
- [5] R. Duncan, F.M. Veronese, PEGylated protein conjugates: a new class of therapeutics for the 21st century, in: F.M. Veronese (Ed.), *PEGylated Protein Drugs: Basic Science and Clinical Applications*, Birkhäuser Verlag, Basel, Switzerland, 2009, pp. 1–9.
- [6] G. Sun, X. Lin, Z. Wang, Y. Feng, D. Xu, L. Shen, PEGylated inulin as long-circulating pharmaceutical carrier, *J. Biomater. Sci. Polym. Ed.* 22 (2011) 429–441.
- [7] K.M. Huh, T. Ooya, W.K. Lee, S. Sasaki, I.C. Kwon, S.Y. Jeong, N. Yui, Supramolecular-structured hydrogels showing a reversible phase transition by inclusion complexation between poly(ethylene glycol) grafted dextran and α -cyclodextrin, *Macromolecules* 34 (2001) 8657–8662.
- [8] A.N. Lukyanov, R.M. Sawant, W.C. Hartner, V.P. Torchilin, PEGylated dextran as long-circulating pharmaceutical carrier, *J. Biomater. Sci. Polym. Edn.* 15 (2004) 621–630.
- [9] T.M. Rogge, C.V. Stevens, A. Vandamme, K. Booten, B. Levecke, C. D'Hooge, B. Haelterman, J. Corthouts, Application of ethoxylated inulin in water-blown polyurethane foams, *Biomacromolecules* 6 (2005) 1992–1997.
- [10] S. Wang, Z. Zhang, X. Lin, D.S. Xu, Y. Feng, K. Ding, A polysaccharide, MDG-1, induces S1P₁ and bFGF expression and augments survival and angiogenesis in the ischemic heart, *Glycobiology* 20 (2010) 473–484.
- [11] Q. Zheng, Y. Feng, D.S. Xu, X. Lin, Y.Z. Chen, Influence of sulfation on anti-myocardial ischemic activity of *Ophiopogon japonicus* polysaccharide, *J. Asian Nat. Prod. Res.* 11 (2009) 306–321.
- [12] X. Lin, D.S. Xu, Y. Feng, L. Shen, Determination of *Ophiopogon japonicus* polysaccharide in plasma by HPLC with modified postcolumn fluorescence derivatization, *Anal. Biochem.* 342 (2005) 179–185.
- [13] X. Lin, S. Wang, Y. Jiang, Z.J. Wang, G.L. Sun, D.S. Xu, Y. Feng, L. Shen, Poly(ethylene glycol)-Radix *Ophiopogonis* polysaccharide conjugates: preparation, characterization, pharmacokinetics and in vitro bioactivity, *Eur. J. Pharm. Biopharm.* 76 (2010) 230–237.
- [14] X. Lin, Z. Wang, G. Sun, L. Shen, D. Xu, Y. Feng, A sensitive and specific HPGPC-FD method for the study of pharmacokinetics and tissue distribution of Radix *Ophiopogonis* polysaccharide in rats, *Biomed. Chromatogr.* 24 (2010) 820–825.
- [15] M. Rodriguez, W.J. Cai, S. Kostin, B.R. Lucchesi, J. Schaper, Ischemia depletes dystrophin and inhibits protein synthesis in the canine heart: mechanism of myocardial ischemic injury, *J. Mol. Cell. Cardiol.* 38 (2005) 723–733.
- [16] A.N. Lukyanov, W.C. Hartner, V.P. Torchilin, Increased accumulation of PEG-PE micelles in the area of experimental myocardial infarction in rabbits, *J. Control. Release* 94 (2004) 187–193.
- [17] D.S. Xu, Y. Feng, X. Lin, H.L. Deng, J.N. Fang, Q. Dong, Isolation, purification and structural analysis of a polysaccharide MDG-1 from *Ophiopogon japonicus*, *Acta Pharmaceut. Sin.* 40 (2005) 636–639.
- [18] T.N. Palmer, V.J. Caride, M.A. Caldecourt, J. Twickler, V. Abdullah, The mechanism of liposome accumulation in infarction, *Biochim. Biophys. Acta* 79 (1984) 363–368.
- [19] J.K. Armstrong, The occurrence, induction, specificity and potential effect of antibodies against poly(ethylene glycol), in: F.M. Veronese (Ed.), *PEGylated Protein Drugs: Basic Science and Clinical Applications*, Birkhäuser Verlag, Basel, Switzerland, 2009, pp. 147–168.
- [20] R. Webster, E. Didier, P. Harris, N. Siegel, J. Stadler, L. Tilbury, D. Smith, PEGylated proteins: evaluation of their safety in the absence of definitive metabolism studies, *Drug Metab. Dispos.* 35 (2007) 9–16.
- [21] R. Webster, V. Elliott, B.K. Park, D. Walker, M. Hankin, P. Taupin, PEG and PEG conjugates toxicity: towards an understanding of the toxicity of PEG and its relevance to PEGylated biologicals, in: F.M. Veronese (Ed.), *PEGylated Protein Drugs: Basic Science and Clinical Applications*, Birkhäuser Verlag, Basel, Switzerland, 2009, pp. 127–146.
- [22] M.W. Modi, J.S. Fulton, D.K. Buckmann, Clearance of PEGylated (40 kDa) interferon alfa-2a (PEGASYS) is primarily hepatic, *Hepatology* 32 (2000) 371A.
- [23] A. Bendele, J. Seely, C. Richey, G. Sennello, G. Shopp, Short communication: renal tubular vacuolation in animals treated with polyethylene-glycol-conjugated proteins, *Toxicol. Sci.* 42 (1998) 152–157.
- [24] G.L. Sun, X. Lin, Mechanisms and strategies for targeting drugs to myocardial ischemic regions, *Acta Pharm. Sin.* 45 (2010) 827–832.
- [25] V.P. Torchilin, Targeting of drugs and drug carriers within the cardiovascular system, *Adv. Drug Deliv. Rev.* 17 (1995) 75–101.
- [26] R.C. Scott, D. Crabbe, B. Krynska, R. Ansari, M.F. Kiani, Aiming for the heart: targeted delivery of drugs to diseased cardiac tissue, *Expert Opin. Drug Deliv.* 5 (2008) 459–470.